University of Szeged

Faculty of Pharmacy

Institute of Pharmaceutical Technology and Regulatory Affairs

Head: *Prof. Dr. habil. Ildikó Csóka PhD*

PhD Thesis

Development of lipid- and polymer-based nanocarriers for intranasal application

By

Hussein Akel

Supervisors:

Prof. Dr. habil. Csóka Ildikó PhD

SZEGED
2022

University of Szeged
Doctoral School of Pharmaceutical Sciences
Head: Prof. Dr. Judit Hohmann D.Sc
Educational Program: Pharmaceutical Technology
Head: Prof. Dr. Ildikó Csóka Ph.D.
Superviser: Prof. Dr. Ildikó Csóka Ph.D.

Hussein Akel

DEVELOPMENT OF LIPID- AND POLYMER-BASED NANOCARRIERS FOR INTRANASAL APPLICATION

Complex Exam Committee:

Head: Prof. Dr. Piroska Szabó-Révész D.Sc., Institute of Pharmaceutical Technology and Regulatory Affairs, University of Szeged

Members: Prof. Dr. Ildikó Bácskay, Department of Pharmaceutical Technology, University of Debrecen

Dr. habil Zoltán Aigner Ph.D., Institute of Pharmaceutical Technology and Regulatory Affairs, University of Szeged

Reviewer Committee:

Head: Prof. Dr. Judit Hohmann D.Sc., University of Szeged, Faculty of Pharmacy Department of Pharmacognosy

Reviewers: Dr. Péter Doró, Ph.D., University of Szeged, Faculty of Pharmacy Institute of Clinical Pharmacy

Dr. György Tibor Balogh, D.Sc., Budapest University of Technology and Economics, Department of Chemical and Environmental Process Engineering,

Members: Prof. Dr. István Szatmári D.Sc., University of Szeged, Faculty of Pharmacy Institute of Pharmaceutical Chemistry

Secretary: Dr. Renáta Kanizsai-Minorics, Ph.D., University of Szeged, Faculty of Pharmacy Institute of Pharmacodynamics and Biopharmacy

SZEGED

2022

ABBREVIATIONS

CNS	central nervous system	**MEL**	meloxicam
AD	Alzheimer's disease	**Ins**	Insulin
BBB	blood-brain barrier	**QbD**	Quality by Design
SLNs	solid-lipid nanoparticles	**RA**	risk assessment
PLGA	Poly lactic-co-glycolic acid	**CSF**	cerebrospinal fluid
NPs	Nanoparticles	**QTPP**	quality target product profile
C-NPs	chitosan coated nanoparticles	**CPPs**	critical process parameters
C-SLNs	chitosan coated SLNs	**CMAs**	critical material attributes
C-PLGA NPs	chitosan coated PLGA NPs	**CQAs**	critical quality attributes
EMA	European Medicines Agency	**SEM**	scanning electron microscopy
FDA	U.S. Food and Drug Administration	**FTIR**	Fourier transform infrared
MBE	mucin binding efficacy	**XRPD**	X-Ray Powder Diffraction
PDI	poly dispercity index	**ZP**	Zeta potential
API	active pharmaceutical ingredient	**EE**	encapsulation efficacy
SNES	simulated nasal electrolyte solution	**DL**	drug load
NSAIDs	non-steroidal anti-inflammatory drugs	**APOE**	ε4 apolipoprotein E

1. INTRODUCTION

Neurodegeneration is an umbrella term for a scope of disorders that primarily influence the neurons in the human central nervous system (CNS). It results in problems either with the movement, called ataxias, or with mental functioning called dementias. Dementias are considered the tremendous burden of neurodegenerative diseases, with Alzheimer's disease (AD) representing approximately 60-70% of the cases worldwide. All the available remedies for AD are of short-time efficacy accompanied by severe side effects. They help only managing the symptoms with no disease-modifying properties and follow the conventional oral administration. The intranasal route has emerged as an alternative pathway offering a non-invasive way for drug delivery to the CNS, enabling self-administration, good bioavailability, slow drug metabolism, and evading the first-pass metabolism. Nanotechnology is a revolutionary way of introducing the APIs intranasally for the brain delivery as they fulfill the requirements of bypassing the blood-brain barrier (BBB). Among the nanoparticles, Solid lipid nanoparticles (SLNs) and Poly lactic-co-glycolic acid (PLGA) are preferable for the N2B delivery of pharmaceutics as they are inert, non-toxic, submicron colloidal carriers with an ideal particle size range. Moreover, they control the drug release properties and are suitable for both the hydrophobic and hydrophilic APIs showing low toxicity and good biocompatibility& biodegradability. Since SLNs and PLGA NPs are sophisticated systems, relevant guidelines must be applied during all their manufacturing stages. Furthermore, the FDA has intensified the application of the Quality by Design (QbD) methodology, which can be remarkably useful for the novel, high-risk dosage forms, and administration routes for careful planning and development even at the early phase of the research.

This research was conducted to assess the potentiality of the above-mentioned two types of nanoparticles to ameliorate the brain delivery of meloxicam as a non-biological API and insulin as a biological one. The work adopted the QbD methodology to optimize the formulation materials and process parameters. Meloxicam was chosen because numerous epidemiological studies suggest that long-term use of non-steroidal anti-inflammatory drugs (NSAIDs) may protect subjects carrying one or more ε4 allele of the apolipoprotein E (APOE ε4) against the onset of AD. However, the high plasma protein binding and low apparent distribution volumes of MEL decrease its pharmacological effect. On the other hand, Insulin, as a biological molecule, showed an

ameliorating effect of intranasal insulin in AD. It helps boosting memory performance as the brain insulin resistance tends to be pathophysiological factor in AD.

2. AIMS

The aim of this study was to develop two nanoformulations (SLNs and PLGA NPs) of meloxicam and insulin for the intranasal application and check their ability to directly deliver the encapsulated active pharmaceutical ingredient (API) to the brain.

- Screening the literature of the nose to brain delivery of pharmaceutics shows the high potential of SLNs and PLGA NPs to be the nanoparticles of choice for the direct delivery of pharmaceutical molecules to the brain following the intranasal application.
- The applicability of SLNs and PLGA NPs in a nasal formulation is considered a novel approach in pharmaceutical technology, thus, limited data for such systems are available up till the moment.
- QbD approach was employed to get the critical process and material parameters that impact the preparation of nanosuspensions ranked and prioritized.
- Four meloxicam/ insulin-containing nanoformulations were developed as freeze-dried formulations. Introducing nano encapsulated meloxicam/ insulin intranasally for the direct delivery to the brain via nanosystem-based formulations is a novel strategy that could ameliorate the brain bioavailability of both meloxicam and insulin with relatively high patient-acceptance. Then, the prioritized influential parameters were experimentally studied and optimized to finally get the nanosystems.

The main steps in the experiments were the following:

1. Implementation of the QbD approach for the research and development approach of the nanosystems as meloxicam/ insulin-containing preformulations as high potential choices to enhance the brain bioavailability.
2. Getting the optimized nanoformulations by performing the proper experiments and evaluating them regarding their physical, chemical, and characteristic properties.
3. Performing *in vitro* cell line studies, and *in vitro-in vivo* correlation studies of the nanoformulations.

4. MATERIALS

Meloxicam (MEL) was obtained from Egis Pharmaceuticals Ltd. (Budapest, Hungary). Cholesterol was purchased from Molar Chemicals (Budapest, Hungary), while Insulin from the bovine pancreas, phosphatidylcholine (PCL), PLGA (poly (lactic-co-glycolic acid)) 75/25 Mw 4,000–15,000 Da, and poloxamer 188 were purchased from Sigma-Aldrich (Steinheim, Germany). Chitosan, trehalose dihydrate, and all the organic solvents (all are of analytical grade) and reagents were purchased from Merck (Darmstadt, Germany), unless otherwise indicated.

5. METHODS

5.1. Initial Risk Assessment (RA) as a part of QbD

The QTPP of MEL-loaded NPs was defined as the first step of QbD. RA tools were then used to rank CPPs and CMAs that significantly impact the quality (CQAs) of the final MEL loaded NPs. The initial RA was carried out using Lean QbD Software (Lean QbD® Software, QbD Works LLC. USA, CA, Fremont).

5.2. Preparation of MEL SLNs, MEL PLGA NPs, Ins SLNs, and Ins PLGA NPs

Mel and Ins NPs were prepared following a modified double-emulsion solvent-evaporation technique, as shown in the following table, Table 1.

Table 1. Steps and conditions of preparation of the NPs

	MEL NPs	**Ins NPs**
W/O/W emulsion	SLNs: 0.2ml MEL solution/1ml PCL in cyclohexane or cholesterol in ethanol/ 2% w/v poloxamer solution Polymeric NPs: 0.2ml MEL solution/ 1ml (12 mg/ml) PLGA in ethyl acetate or 12 mg/ml PCL in chloroform / 2% poloxamer solution	SLNs: 0.35 ml Ins solution/1ml PCL solution in cyclohexane/ 1.6 mL of 2% w/v poloxamer solution PLGA NPs: 0.35 ml Ins solution/ 1ml (12 mg/ml) PLGA in ethyl acetate solution in cyclohexane/ 1.6 mL of 2% w/v poloxamer solution
Homogenizing condition	0.5 cycles with 75% amplitude	
Solvent evaporation	Stirring over the night at ambient temperature using a magnetic stirrer	
Chitosan coating	After mixing NPs with chitosan solution for two hours, the NPs were centrifuged, purified, and freeze-dried in the presence of 5% trehalose	

5.3. Characterization of NPs

5.3.1. Determination of mean particle diameter, polydispersity index and zeta potential

The mean particle diameter (Z-average), polydispersity index (PDI), and surface charge (zeta potential) of the NPs were analyzed in folded capillary cells, using Malvern Nano zetasizer instrument (Malvern Instruments, Worcestershire, UK). The temperature and refractive index of the apparatus were set at 25 ◦C and 1.755, respectively, with a total number of scans of 17. Samples were diluted with ultrapure water (1:200 v/v) and placed in a cuvette for the analysis. The measurements were repeated three times, data was presented as mean±SD.

5.3.2. Determination of encapsulation efficacy (EE) and drug loading (DL)

The EE and DL of MEL- and Ins-loaded NPs were analyzed by high-pressure liquid chromatography (HPLC) following an HPLC method with the following details:

	Mel NPs	Ins NPs
HPLC system used	the Agilent 1260 HPLC system	the Agilent 1260 HPLC system
Stationary phase	A C18 column (Kinetex® (5 µm, 150 mm × 4.6 mm)	A C18 column (Gemini-NX® C18 150 mm × 4.6 mm, 5 µm)
Sample size	10µl/ 30°C	20µl/ 30°C
Mobile phases	0.065 M KH2PO4 solution adjusted to pH 2.8 with phosphoric acid (A) and methanol (B)	purified water adjusted pH = 2.8, phosphoric acid and acetonitrile in 68:32 ratio
LoD/ LoQ	16/49 ppm	87/26 ppm
Type of elusion	Gradient	Isocratic
UV-Vis spectrum	355 ± 4 nm	280 nm

The EE and DL were calculated by applying the following equations:

$$EE(\%) = \frac{\text{The calculated amount of MEL encapsulated in the freeze dried SLNs}}{\text{total amount of MEL used in the preparation}} \times 100$$

$$DL\ (\%) = \frac{\text{The amount of encapsulated insulin in the freeze} - \text{dried nanoparticles}}{\text{The weight of the freeze} - \text{dried nanoparticles}} \times 100$$

5.3.3. Scanning Electron Microscopy (SEM)

The surface morphology of the NPs was tested using Scanning Electron Microscopy (SEM) (Hitachi S4700, Hitachi Scientific Ltd., Tokyo, Japan) at 10 kV. The samples were coated with

gold–palladium under an argon atmosphere. The air pressure was 1.3–13 mPa. (Bio-Rad SC 502, VG Microtech, Uckfield, UK).

5.3.4. Fourier-Transform Infrared Spectroscopy (FT-IR)

The compatibility was investigated between the drug and the used excipients by a Thermo Nicolet AVATAR FT-IR spectrometer (Thermo-Fisher, Waltham, USA). FTIR spectra of pure components, PLGA NPs, and SLNs were measured as follows: each component was placed along with 150 mg KBr powder, the wavenumber range set on 4000-400 cm^{-1} at a resolution of 4 cm^{-1} before running the measurement.

5.3.5. X-ray Powder Diffraction (XRPD)

The physical nature and interactions were inspected between the drug and the used excipients by a BRUKER D8 Advance X-ray powder diffractometer (Bruker AXS GmbH, Karlsruhe, Germany). The X-ray powder diffractograms of the pure MEL, excipients, uncoated, and coated NPs were obtained in the angular range of 3–40° 2θ at a step time of 0.1 s and a step size of 0.007° at ambient temperature.

5.4. In vitro evaluation of the prepared nanosystems

5.4.1. In vitro drug release test

A dialysis bag diffusion technique was employed to investigate the drug release behavior of both MEL-NPs and Ins-NPs at nasal conditions, the modified paddle method (Hanson SR8 Plus, Teledyne Hanson Research, Chatsworth, CA, USA). In case of MEL-NPs 10 mg of MEL and precise aliquots of MEL-NPs equivalent to 10 mg were placed into dialysis bags with a 12–14 kDa cut-off (Spectra/Por® Dialysis Membrane, Spectrum Laboratories Inc., Rancho Dominguez, CA, USA) and hermetically sealed. The sealed bags were then immersed in dissolution vessel containing volume of 100 ml phosphate buffer (pH 7.4) and left to agitate at 50 rpm at 35°C. The sampling process was executed by withdrawing aliquots from the release medium at pre-established periods up to 6 h and replacing them with an equivalent volume of the fresh medium to maintain the ‘sink’ condition. Both Ins and MEL content was analyzed using HPLC for. The results were reported as means ± SD.

5.4.2. Mucoadhesion test

Mucoadhesion was determined using two coordinated methods: the direct method (turbidimetric method) and the indirect method (Measuring the ZP changes). The direct method was carried out

as follows: briefly, equal volumes of NPs suspensions in simulated nasal electrolyte solution (SNES) and porcine mucin solution 0.05% were mixed and incubated at 37° C, and continuously stirred for 4 h with a pre-determined sampling interval for of 1 h. The centrifugation was then performed at 17,000 rpm at 4° C. The supernatant content of the free mucin was determined at 255 nm using a UV spectrophotometer. The mucin binding efficacy (MBE) can be calculated based on the following equation:

$$\text{MBE} = \frac{\text{Total mucin} - \text{Free mucin}}{\text{Total mucin}} \times 100$$

The mucoadhesive properties were also evaluated by measuring the zeta potential using the Malvern Nano ZS instrument (Malvern Instruments, Worcestershire, UK) through the interaction of negatively charged mucins with SLNs, PLGA NPs, and C-SLNs.

5.4.3. Permeability test

The intranasal suspension of the NPs was placed in the first chamber and considered to be the donor phase; API NPs in 9 ml of SNES. A semi-permeable cellulose membrane (Synthetic membrane PALL Metricel membrane®), previously impregnated in isopropyl myristate for 1 h, was placed between the two chambers as a membrane to imitate the lipophilicity of the nasal mucosa. The acceptor phase was represented by 9 ml of pH 7.4 phosphate buffer. The donor and the acceptor phase volumes were the same (9 ml) and had a 0.69 cm^2 diffusion area. The temperature of the phases was set to 35 °C (Thermo Haake C10-P5, Sigma, Aldrich Co.) to simulate the nasal condition, and the agitation using magnetic stirrers that were set to 50 rpm to mimic the movements of the cilia and the blood circulation. The diffused amount of MEL, Ins and NPs was determined using HPLC, and measurements were implemented in triplicate, results were reported as means ± SD.

5.5. In Vitro Cell Line Studies

5.5.1. Human RPMI 2650 Nasal Epithelial Cell Culture

Human RPMI 2650 nasal epithelial cells were kept in a humidified 37° C incubator with 5% CO2. All the plastic surfaces were coated with 0.05% collagen in sterile distilled water before cell seeding in culture dishes, and the medium was changed every 2 days. The cells were trypsinized with 0.05% trypsin 0.02% EDTA solution when they reached about 80–90% confluency in the dishes. To induce tighter epithelial barrier properties, retinoic acid (10 µM) and hydrocortisone (500 nM) were added to the cells 1 day before the experiment. For the permeability measurements,

RPMI 2650 epithelial cells were co-cultured with human vascular endothelial cells to create a more physiological barrier.

5.5.2. Human hCMEC/D3 Brain Endothelial Cell Line

Cultures of hCMEC/D3 cells (≤ P35) were grown in MCDB 131 medium (Pan-Biotech, Aidenbach, Germany) supplemented with 5% FBS, GlutaMAX (100×, Life Technologies, Carlsbad, CA, USA), lipid supplement (100×, Life Technologies, Carlsbad, CA, USA), 10 ng/mL ascorbic acid, 550 nM hydrocortisone, 100 ng/mL heparin, 1 ng/mL basic fibroblast growth factor (bFGF, Roche, San Francisco, CA, USA), 2.5 μg/mL insulin, 2.5 μg/mL transferrin, 2.5 ng/mL sodium selenite (ITS), and 50 μg/mL gentamicin. All the plastic surfaces were coated with 0.05% collagen in sterile distilled water before cell seeding and the medium was changed every 2 days. Before each experiment, the medium of hCMEC/D3 cells was supplemented with 10 mM LiCl for 24 h to improve the barrier properties.

5.5.3. Cell Viability Measurement

The kinetics of the epithelial and endothelial cell reaction to the different treatments were monitored by impedance measurement at 10 kHz (RTCA-SP instrument, Agilent, Santa Clara, CA, USA). The impedance measurement is label-free, non-invasive, and correlates linearly with the adherence, growth, number, and viability of cells in realtime. For background measurements, the 50 μL cell culture medium was added to the wells. Then, the cells were seeded at a density of 2×10^4 RPMI 2650 cells/well and 6×10^3 hCMEC/D3 cells/well in 96-well plates coated with integrated gold electrodes (E-plate 96, Agilent, Santa Clara, CA, USA). The cells were cultured for 5–7 days in a CO2 incubator at 37° C and monitored every 10 min until the end of experiments. In addition, the cells were treated at the beginning of the plateau phase of growth. The insulin, insulin NPs, and HCl solution were diluted in a cell culture medium and the effects were followed for 20 h. Triton X-100 detergent (1 mg/mL) was used as a reference compound to induce cell toxicity.

5.5.4. Permeability Studies

For the permeability experiments, the inserts were transferred to 12-well plates containing 1.5 mL Ringer-HEPES buffer in the acceptor (lower/basal) compartments. In the donor (upper/apical) compartments, 0.5 mL buffer was pipetted containing insulin alone or encapsulated formulations. To avoid the unstirred water layer effect, the plates were kept on a horizontal shaker (120 rpm)

during the assay. The assays lasted for 60 min. Samples from both compartments were collected and the insulin concentration was measured by HPLC. The apparent permeability coefficients (P_{app}) were calculated as described previously. Briefly, the cleared volume was calculated from the concentration difference of the tracer in the acceptor compartment (Δ[C]A) after 60 min and in donor compartments at 0h ([C]D), the volume of the acceptor compartment (VA; 1.5 mL), and the surface area available for permeability (A; 1.12 cm^2) using this equation:

$$P_{app}\left(\frac{cm}{s}\right) = \frac{\Delta[C]_A \times V_A}{A \times [C]_D \times \Delta t}$$

6. RESULTS AND DISCUSSION

6.1. Initial Risk Assessment (RA) as a part of QbD

Risk assessment was conducted to rank and prioritize the factors that highly impact the final product quality. The QbD-based risk assessment started by setting the QTPPs encompassing the desired quality attributes in MEL- and Ins-loaded NPs. The following step was to create an Ishikawa fishbone diagram that summarizes the risk analysis process. It clarifies the cause-effect relationship between the significant variables and the CMAs, CQAs, and CPPs of the nanoformulations (**Figure 1**). This diagram is considered an efficient quality management tool aids in exploring the cause-effect relationship.

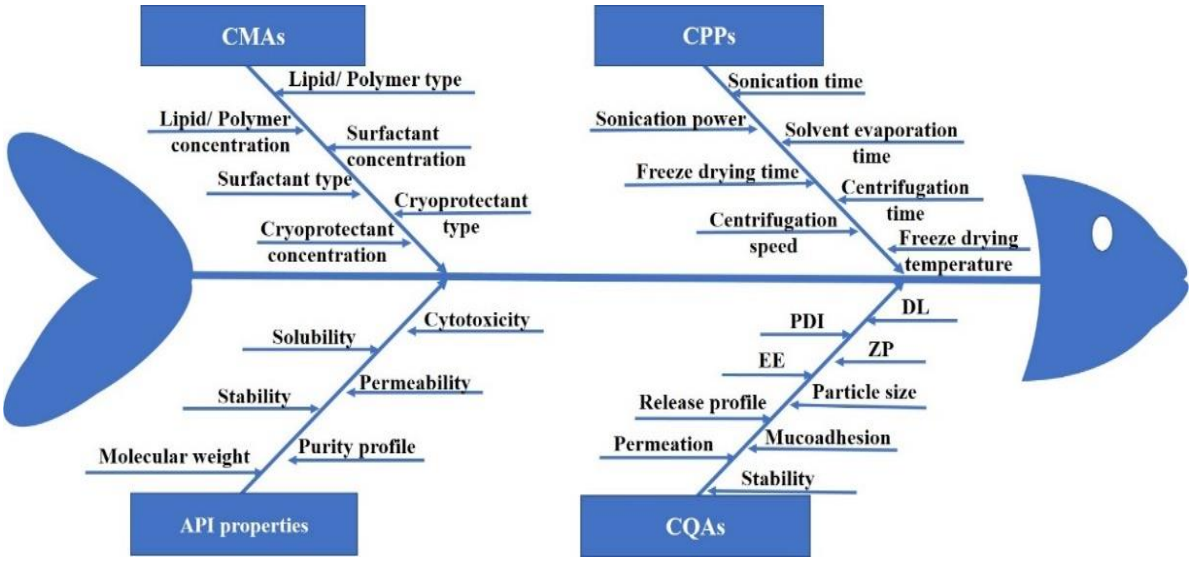

Figure 1. Ishikawa diagram illustrating the risk factors for the nose-to-brain delivery of MEL/ INS-loaded NPs.

This was followed by an initial RA of the CQAs, which were namely: average hydrodynamic diameter (Z-average), zeta potential, PDI, EE, dissolution rate, mucoadhesion, and permeability using Lean QbD software. After that, the evaluation of the selected CMAs and CPPs took place that was based on the thoroughly analyzed relevant literature and the results of experimental research work in addition to the proper prior knowledge. The risk assessment of the highest risky CPPs and CMAs affecting the quality of both SLNs and PLGA NPs for the IN application with the aim of the direct nose to brain delivery demonstrated that the vastly influential CPP was sonication time. In contrast, the immensely influential CMAs were lipid/ polymer type, lipid/ polymer concentration, surfactant type, and surfactant concentration.

6.2. Characterization of NPs

6.2.1. Mean particle diameter, size distribution, and zeta potential

Both types of NPs, in addition to the coated one, comply with the size requirement of nasal administration for the brain targeting, which preferred to be up to 200 nm. PDI values were lower than 0.3 for all formulations indicating monodisperse size distributions. That is in accordance with the SEM images (**Figure 2**), which demonstrate the NPs homogenized dispersion.

The zeta potential values of PLGA NPs and SLNs were negative, which is logical due to the negative charge of phosphatidylcholine approximated in a range of -10 and -30 mV at the neutral pH owing to the presence of phosphate and carboxyl groups, in contrast with the negatively charged carboxyl groups on PLGA that are the only cause behind the negative charge. As expected, the chitosan coating leads to a charge shifting to become positive due to the electrostatic interactions, which suggest appropriate adsorption of the positively charged polymer (chitosan) onto the surface of the NPs.

6.2.2. Encapsulation efficacy and Drug Load:

The encapsulation efficacy (EE) and drug loading (DL) were not significantly higher ($p > 0.05$) in the case of SLNs than PLGA NPs, which could be explained by the ability of phosphatidylcholine particles to entrap meloxicam and insulin molecules into the Ins SLNs by forming hydrogen bonds employing the three available electron pairs in each unit, whilst in the case of Ins PLGA NPs these electron pairs are used to attach the lactic-co-glycolic units with each other as described in our previous research work. Furthermore, coating the NPs with chitosan seems to be a beneficial tool

in getting higher EE and DL due to the formation of an impermeable coating that offers protection against the leakage of insulin molecules from the prepared NPs.

6.2.3. Scanning Electron Microscopy (SEM)

Scanning electron microscopy (SEM) images of the obtained NPs showed spherical shape with a smooth surface, which provides better dissolution, mucoadhesion, and permeation than the needle- or disk-like shape NPs (**Figure 2**). Moreover, the spherical shape of the NPs will result in a minimal membrane bending energy, therefore higher stability and lower chance of entrapped drug leakage compared with the non-spherical counterparts that involve a strong membrane deformation, higher friction and consume energy.

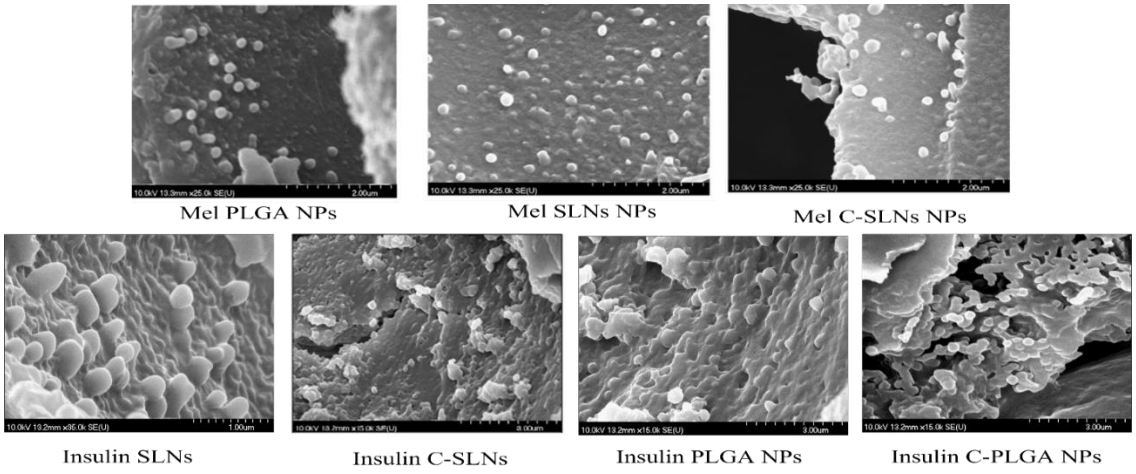

Figure 2. SEM images representing the resulted NPs. The images show the spherical shape and well dispersed NPs with preferable nano-size

6.2.4. Fourier-Transform Infrared Spectroscopy (FT-IR)

The FT-IR spectra of MEL, both loaded NPs formulations, and the used excipients are presented in **Figure 3**.

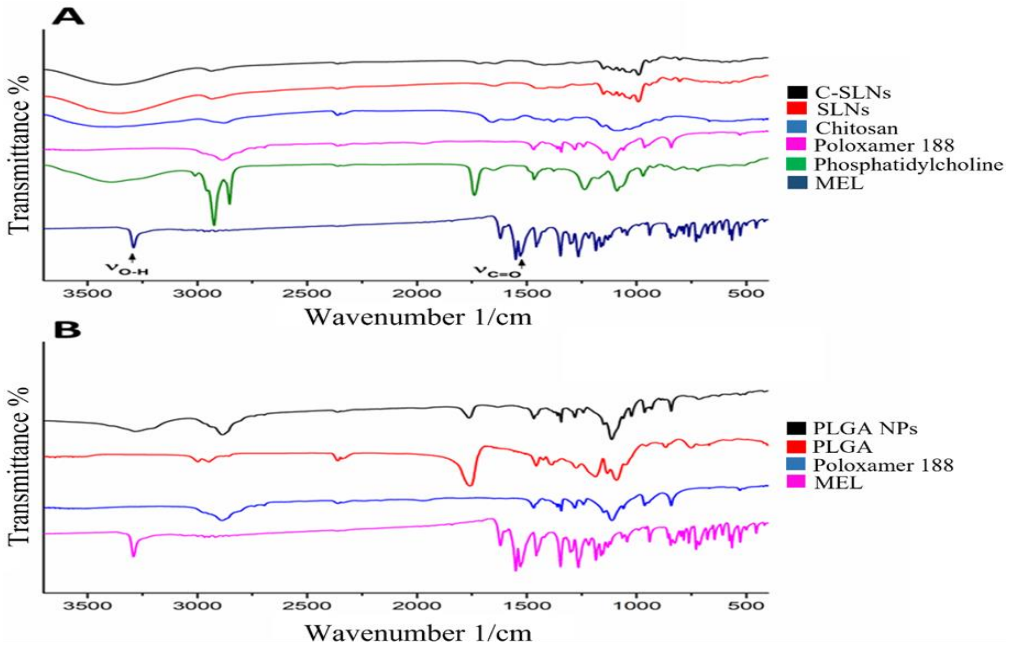

Figure 3. FTIR spectra of MEL, MEL SLNs, MEL C-SLNs, Mel PLGA NPs, and the used excipients

The FT-IR spectra of the NPs showed no changes in the MEL chemical structure and presented no significant difference in the main functional groups of MEL. The absorption band at 3290 cm^{-1} related to the hydroxyl group attached to an aromatic ring of MEL; furthermore, the carbonyl group vibration at 1550 cm^{-1} is not visible in the spectrum of C-SLNs. These characteristic peaks fading points out H-bonding formation between SLN and chitosan, which proves that the coating process was achieved.

6.2.5. X-ray Powder Diffraction (XRPD)

An overlay of powder XRPD patterns of MEL, SLNs, C-SLNs, PLGA NPs, and the used excipients is depicted in **Figure 4**.

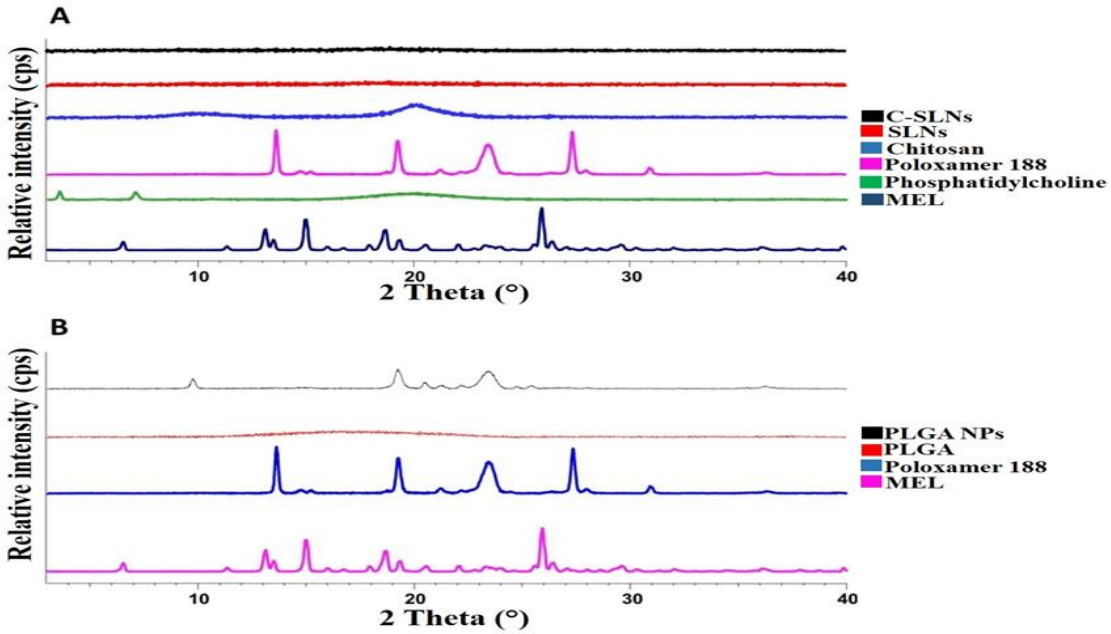

Figure 4. XRPD spectra of SLNs and C-SLNs (A), PLGA NPs (B), and the used excipients

The XRPD of the MEL shows characteristic peaks to its crystalline structure. However, SLNs, C-SLNs, and PLGA NPs did not show the MEL characteristic peaks in their XRPD pattern. This confirms the successful encapsulation of the API into the NPs. The previous results are conforming to the results of FTIR, encapsulation efficacy, and drug loading.

6.3 In vitro evaluation of the prepared nano systems

6.3.1. Mucoadhesion test

The mucoadhesion test was performed to understand the behavior of the NPs towards the mucin, which forms the main component of the nasal mucosa, and the higher the mucoadhesion, the better the retaining of the NPs adsorbed to the nasal mucosa. Based on **Figure 5**, it can be noticed that the highest mucoadhesion could be achieved when formulating the C-NPs followed by the uncoated SLNs then the PLGA NPs.

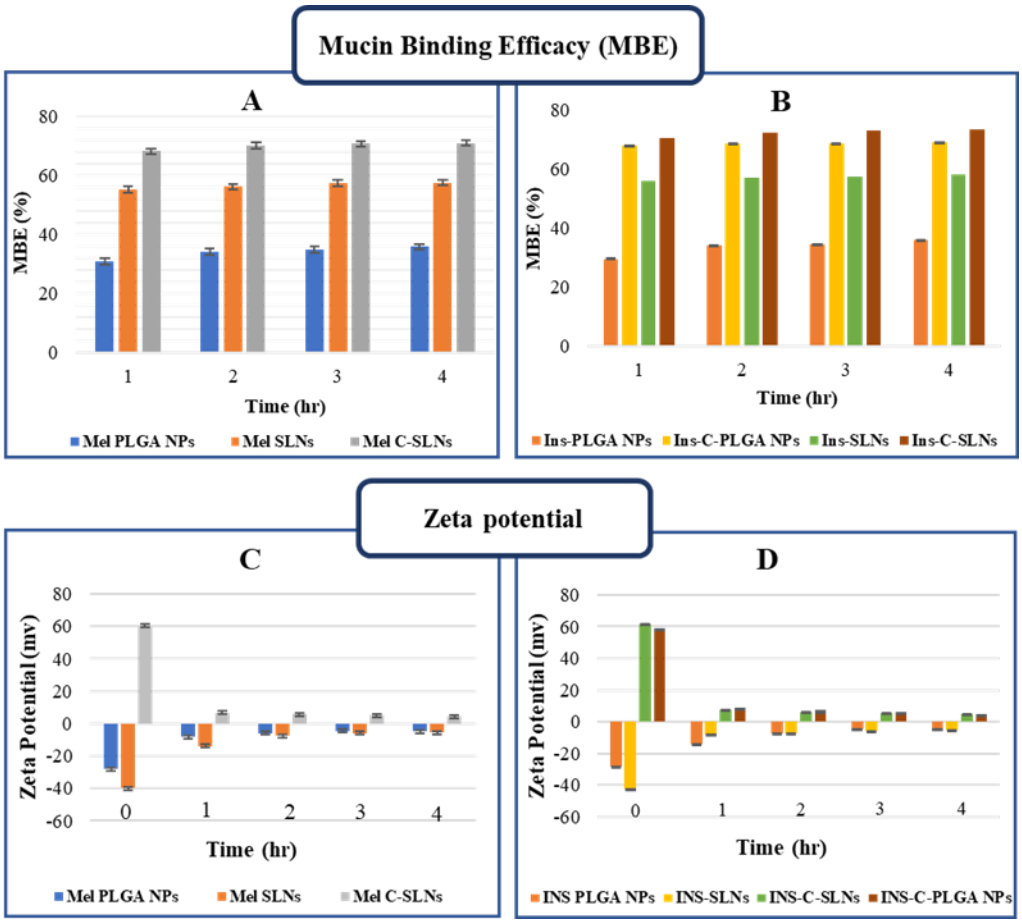

Figure 5. Mucoadhesion assay of MEL and Ins NPs, where A represents ZP analysis method for MEL NPs, B represents ZP analysis method for Ins NPs, C represents Turbidity analysis method for MEL NPs, and D represents Turbidity analysis method for Ins NPs. Measurements were done in triple (n=3 independent formulations), and data are represented as means ± SD.

In the turbidimetric method, the mucoadhesive strength was estimated by calculating mucin binding efficacies to the obtained NPs. The mucin binding efficacy MBE of MEL-PLGA NPs, MEL-SLNs, and MEL-C-SLNs were 36.55%, 57.59%, and 71.09%, respectively, while the MBE for Ins SLNs and Ins PLGA NPs were 35.99% and 58.2%, respectively, which were increased by the chitosan coating to 69.14% and 73.45% by the end of the experiment, as **Figure 5A** and **5B** represent. Since the mucin possesses a negative charge along with its glycosylated structure, the positively charged C-NPs will have significantly higher interaction with it than the negatively charged SLNs and PLGA NPs. The first leads to formulating ionic bonds, while the latter occurs by forming electrostatic interactions ($p<0.05$). In the zeta potential method, the zeta potential variation values were measured up to 4 hours (**Figure 5C** and **5D**). The high positive charge of the

C-NPs led to a significant neutralization in the negative charge of mucin ($p<0.05$), which may happen by the formation of the ionic bonds. On the other hand, uncoated SLNs and PLGA NPs remained negative; thus, the interaction with mucin happens weakly with insignificant charge changes. ($p>0.05$). The ZP method results are consistent with those achieved by the turbidity method, as the total changes in ZP values match the MBE of each type of NPs. Both methods demonstrated higher mucoadhesion of the APIs C-SLNs followed by the APIs SLNs, which were superior to the PLGA NPs.

6.3.2. Dissolution test

The in vitro dissolution profiles of pure MEL and MEL-loaded NPs were investigated in intranasal-simulated conditions, using simulated nasal electrolytic solution (SNES) medium (pH of 5.6), and the results are presented in **Figure 6A**, while the dissolution behavior of the Ins and Ins NPs was investigated under CSF and systemic circulation conditions to simulate the drug release after nasal absorption, where native insulin was used as a reference, and PBS (pH = 7.4) was employed as the dissolution medium. **Figure. 6B** represents the results of Ins dissolution test.

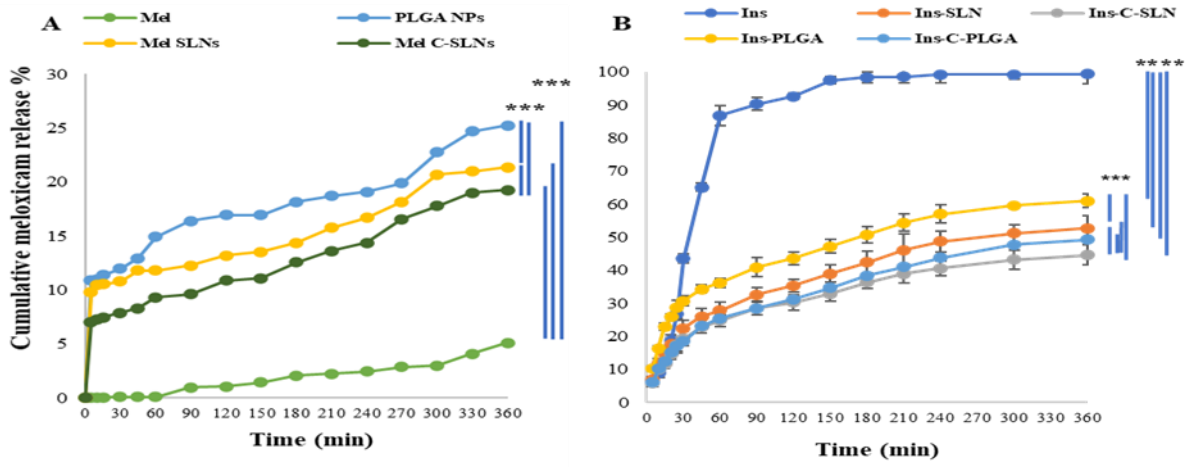

Figure 6. *In vitro dissolution behavior of the native APIs and the prepared NPs, where A represents MEL and B represents Ins. Measurements were done in triple (n=3 independent formulations), and data are represented as means ± SD.*

It is evident that pure MEL demonstrates a modest solubility (5.10 ± 0. 9 µg/mL, over 360 min, at 35°C) due to its chemical structure and because of the weak acidic character resulted in this medium (pKa= 3.43); fabrication of MEL in nanoformulations indicated a significant increase ($p<0.001$) in the dissolution rate compared to pure MEL (approximately 4-5 times higher). The release behavior from the NPs demonstrated a sustained release pattern. This begins with a

moderate early rapid release over the first hour, where 12.94 ± 0.86%, 11.79± 0.74 of MEL were released from the PLGA NPs and SLNs, respectively. The previous has been frequently reported for PLGA NPs and SLNs. This moderate initial burst effect may be due to the surface-adsorbed drug particles on the NPs in addition to the drug molecules that are placed near the surface having poor links to the NPs system. A slow-release profile followed this until 6 h, where only 25.26 ± 2.39%, 21.37 ± 1.47 of cumulative MEL release was observed for PLGA NPs and SLNs, respectively ($p < 0.05$) since the encapsulated drug was slowly diffused out of the NPs core. The previous results point out that a significant part of the drug was kept encapsulated into the NPs after being surrounded by nasal mimetic conditions. Thus, it can be released into the targeted position.

Turning to insulin case, the native insulin demonstrated the highest dissolution rate among the tested formulations in PBS, which can be related to the isoelectric point of bovine insulin. The applied insulin has an isoelectric point of 5.3-5.4, therefore the application of a medium with a pH value below 4 or above 7 will lead to an enhanced solubility. Moreover, encapsulation of insulin in Ins SLNs and Ins PLGA NPs was significantly accompanied ($p < 0.001$) by 2-folds and 1.67-fold decreasing in the dissolution rate of insulin respectively, which can be explained by the controlled release properties of the lipid and polymeric NPs. Ins PLGA NPs showed significantly higher ($p < 0.05$) drug release in comparison to Ins SLNs, which can be explained by the higher lipophilicity, therefore higher drug retention in case of SLNs. Further coating the NPs with chitosan resulted in a significant slower release compared to the uncoated ones ($p<0.05$), which might be explained by the additional controlling release properties presented by the additional polymer layer of chitosan, classified as a water-insoluble polymer at the physiological pH.

6.4. In Vitro Cell Line Studies for Ins NPs

6.4.1. Permeability Studies through the Human RPMI 2650 Nasal Epithelial Cell Culture

The permeability of insulin was tested on the nasal epithelial and brain endothelial cell barrier models (**Figure 7**).

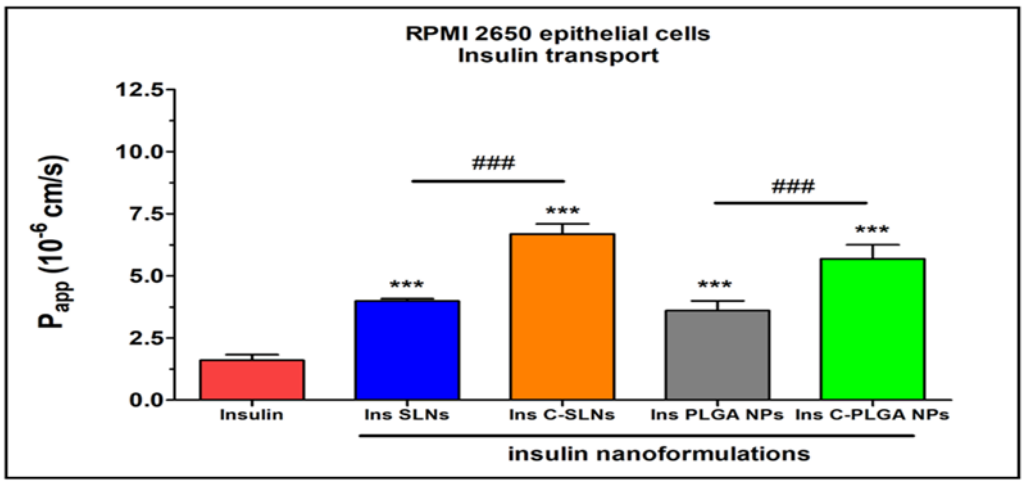

Figure 7. Apparent permeability coefficients (P_{app}) for insulin (0.07 mg/ml in all samples) when applied alone or in different formulations measured across RPMI 2650 epithelial cell layers after 1 hour incubation. Values are presented as means ± SD, n = 4. Statistical analysis: ANOVA followed by Bonferroni test. *** $p < 0.001$ compared to the insulin group, ### $p < 0.01$ compared between the indicated groups.

The results of the *in vitro* cell lines nasal permeability test confirmed the previously performed *in vitro* tests that the transport of insulin was lower in the case of the SLNs, and the PLGA-NP (P_{app}: $\leq 5 \times 10^{-6}$ cm/s) compared to the chitosan-coated NPs. The permeability coefficients of the chitosan-coated NPs were $\geq 6 \times 10^{-6}$ cm/s on both models (**Figure 7** and **8**). The reason for this effect is due to the unique biological properties of chitosan. Chitosan is a linear cationic polysaccharide that is among others non-toxic, biodegradable, and has antibacterial and antimicrobial activity, furthermore, it can enhance the paracellular permeability of biological barriers by modulating tight junction proteins. In the case of the nasal epithelial barrier model, the NPs showed significantly higher permeability (1 to 4-fold) than insulin alone, therefore the NPs increased the flux of insulin through the nasal barrier.

6.4.2. Human hCMEC/D3 Brain Endothelial Cell Line

The brain endothelial barrier model showed high permeability for free insulin compared to the NPs (**Figure 8**).

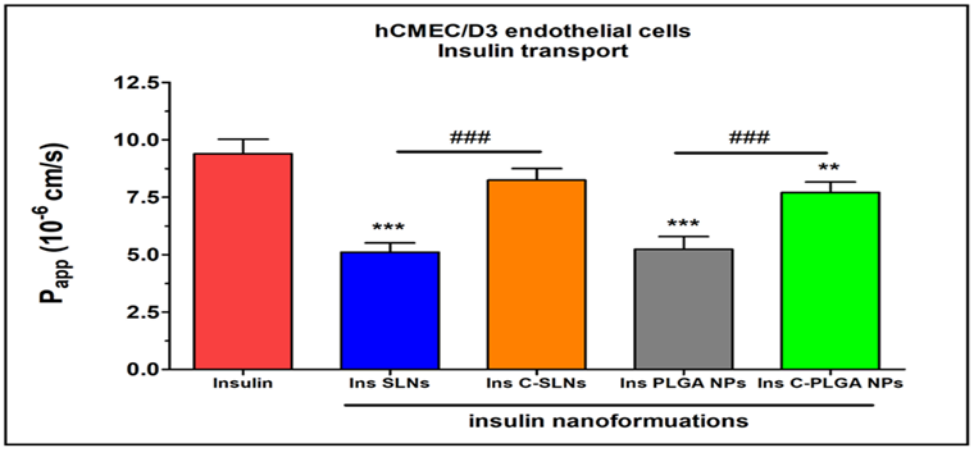

Figure 8. Apparent permeability coefficients (P_{app}) for insulin (0.07 mg/ml in all samples) when applied alone or in different formulations measured across hCMEC/D3 endothelial cell layers after 1 hour incubation. Values are presented as means ± SD.

The difference in the insulin permeability between the two types of barrier models was almost one order to magnitude. The permeability coefficient was 1.6×10^{-6} for insulin in the case of the nasal barrier model and 9.4×10^{-6} for the blood-brain barrier model. The reason for this difference could be the physiological function of these barriers. Insulin, as a hormone, has an important role in blood glucose level regulations in the brain; therefore, the brain endothelial cells contain the highest level of insulin receptors in the human body. The high insulin receptor expression in hCMEC/D3 cells was verified in a quantitative proteomic study.

6.4.3. Cell Viability Measurement

The impedance measurement is a sensitive method for detecting the cellular effects in real-time. Neither RPMI 2650 epithelial cells nor D3 endothelial cells showed notable cell damage after treatments with insulin and insulin-containing NPs (**Figure 9** and **10**).

As a comparison, the reference compound Triton X-100 detergent caused cell death, as reflected by the decrease in impedance in both cell types (**Figure 9A** and **10A**), moreover it shows the kinetics of the cellular effects of treatment solutions, while the columns on **Figure 9B** and **10B** show the effect of insulin and encapsulated NPs at the 1-hour time point.

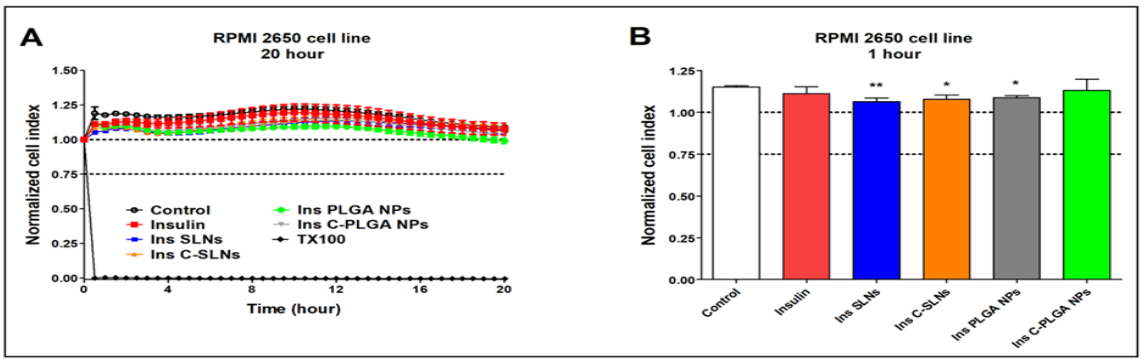

Figure 9. Cell viability of RPMI 2650 nasal epithelial cells after treatment with insulin, insulin NPs, and HCl measured by impedance. The kinetic curve of cell viability during the 20-hour treatment (A) and at the 1-hour time point of the treatment (B). Values are presented as means ± SD.

The kinetic curves of the NPs ran similarly to the untreated control group during the treatment in both epithelial and endothelial models (**Figure 9A** and **10A**). In the case of the hCMEC/D3 cells a slight decrease in cell index values could be observed in two NPs groups (Ins PLGA-NPs and Ins C-PLGA-NPs), however, the cell index values remained above 0.75, which refers to a non-toxic range. The significant differences observed at both cell types (**Figure 9B** and **10B**) at the 1-hour time point are due to the extremely low standard deviation and not because of the toxic effect of treatments.

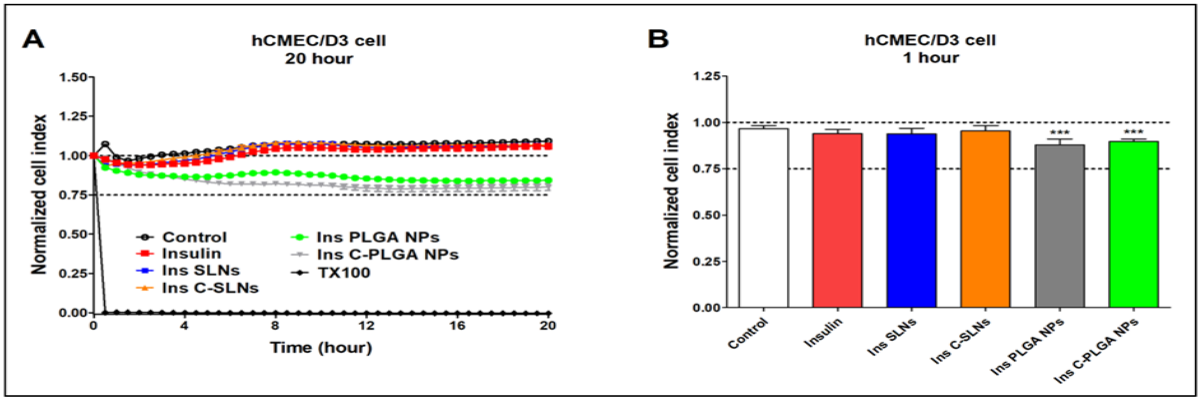

Figure 10. Cell viability of hCMEC/D3 endothelial cells after treatment with insulin, Ins NPs, and HCl measured by impedance. The kinetic curve of cell viability during the 20-hour treatment (A) and at the 1-hour time point of the treatment (B). Values are presented as means ± SD**.**

7. **CONCLUSIONS**

In this study, the QbD concept was successfully employed to thoroughly understand and optimize the process parameters affecting the CQAs when developing nanoformulations for N2B delivery after the IN application.

Compared to MEL PLGA NPs, MEL SLNs showed smaller particle size, higher EE and DL while showing a better-sustained release profile. Moreover, the coating with chitosan showed a superior sustaining release behavior over the uncoated NPs. The mucoadhesion properties of C-MEL-SLNs demonstrated 1.25 and 2-fold enhancement over the MEL-SLNs and MEL-PLGA NPs, respectively. The results of *in vivo-in vitro* correlation of MEL NPs confirmed that the "measured" in vitro and "estimated" in vivo characteristics and behavior of PLGA NPs and SLNs are expected to be better than the native MEL.

On the other hand, four types of NPs were formulated successfully (Ins SLNs, Ins PLGA NPs, C-Ins-SLNs, and C-PLGA-NPs) with optimal Z-average and ZP characteristics for the brain-delivery of IN insulin. The *in vitro* tests showed that compared to Ins-PLGA NPs, Ins-SLNs showed lower Z-average, higher EE and DL while ensuring the better insulin sustaining release profile. Moreover, the Ins C-SLNs and Ins C-PLGA NPs showed a promoted sustaining-release behavior and better mucoadhesion properties over the native insulin and the uncoated NPs. Finally, the permeation of the Ins-SLNs and Ins-PLGA NPs was better than the native insulin and was improved by chitosan-coating.

The *in vitro* cell line experiments proved the safety of prepared NPs for the IN application. Furthermore, the permeation of insulin through the nasal mucosa was the highest in the case of C-Ins-SLNs outperforming the C-Ins-PLGA NPs and the uncoated NPs, which were better than the native insulin. On the other hand, the permeability test showed the superiority of the native insulin in brain endothelial barrier model over the prepared NPs, from which the Ins C-SLNs excelled the Ins C-PLGA NPs followed by Ins SLNs, then Ins-PLGA-NPs. Thus, an optimal nose-to-brain formulation can be obtained using a mixture of the native insulin and Ins C-SLNs. The former ensures the rapid effect, and the latter keeps it for a longer time.

Novelty and practical aspects

- The novelty and strength of this research work come from the ability to optimize and harmonize different aspects starting by analyzing the literature, moving to selecting the administration route, then producing meloxicam and insulin in new dosage forms that has not been studied and developed before.
- Implementing QbD aspects justified the selection of the methodologies and significantly promote the recognizability of seizing optimized formulations based on predefined quality and safety aspects.
- Optimization of critical parameters to produce meloxicam and insulin nanoparticles is considered a significant step toward extending the application of double emulsion solvent evaporation method to formulate different APIs as SLNs and PLGA NPs forms. By these findings, this method can compete with the top-down one in the development of potential products for the market.
- This work provides the first reported evidence for the potential of meloxicam and insulin encapsulation in both polymeric and lipid NPs in the IN delivery with significant SLNs superiority, and their properties were further enhanced by coating with the cationic polymer chitosan. Accordingly, a thorough comparison was performed in vitro, followed by selecting the optimized NPs to be a potential carrier for the IN application of insulin, a potential anti AD drug, with the aim of brain-targeting.
- The cell viability tests proofed the safety of the nanoparticles, and the non-toxic effects of the NPs were verified by a permeability assay, which allows the safe application of these nanoparticles especially after demonstrating good permeation properties through the nasal mucosa and the BBB.
- The obtained SLNs and PLGA NPs can be applied intranasally as a lyophilized powder, which proof their budget friendly usage. The application of lyophilized powdered SLNs and PLGA NPs intranasally with the aim of brain targeting is a new approach in pharmaceutical technology.

ACKNOWLEDGEMENTS

This work was supported by the Ministry of Human Capacities, Hungary (Grant TKP-2020), and by the National Research, Development and Innovation Office, Hungary (GINOP 2.3.2-15-2016-00060), projects.

PUBLICATIONS RELATED TO THE SUBJECT OF THE THESIS:

1. **Akel, H.**, Csóka, I., Ambrus, R., Bocsik, A., Gróf, I., Mészáros, M., Szecskó, A., Kozma, G., Veszelka, S., Deli, M.A., Kónya, Z., Katona, G. In Vitro Comparative Study of Solid Lipid and PLGA Nanoparticles Designed to Facilitate Nose-to-Brain Delivery of Insulin. *International Journal of Molecular Sciences*, 22, 13258 (2021). doi:10.3390/ijms222413258.
   IF: 5.924. (D1 Journal)
2. **Akel, H.**, Ismail, R., Katona, G., Sabir, F., Ambrus, R., Csóka, I. A comparison study of lipid and polymeric nanoparticles in the nasal delivery of meloxicam: Formulation, characterization, and in vitro evaluation. *International Journal of Pharmaceutics*, 604, 120724 (2021). doi: 10.1016/j.ijpharm.2021.120724.
   IF: 5.875. (D1 Journal)
3. **Akel H,** Ismail R, Csóka I. Progress and perspectives of brain-targeting lipid-based nanosystems via the nasal route in Alzheimer's disease. *European Journal of Pharmaceutics Biopharmaceutics* 148, 38-53 (2021). doi: 10.1016/j.ejpb.2019.12.014.
   IF: 5.571. (Q1 Journal)